HYDROGEN EMBRITTLEMENT OF 4340 STEEL AS A RESULT OF CORROSION OF POROUS CADMIUM ELECTROPLATE

A THESIS

Presented to

The Faculty of the Graduate Division

by

John George Rinker

In Partial Fulfillment

of the Requirements for the Degree

Master of Science in Metallurgy

Georgia Institute of Technology

June, 1973

HYDROGEN EMBRITTLEMENT OF 4340 STEEL

AS A RESULT OF CORROSION OF POROUS

CADMIUM ELECTROPLATE

Approved:

Dr. Robert F. Hochman, Chairman

Dr. Helen E. Grenga

Dr. Edgar A. Starke, Jr.

Date Approved by Chairman 6/4/73

ACKNOWLEDGMENTS

I wish to thank my thesis advisor, Dr. Robert F. Hochman, for his confidence, encouragement, and patience throughout the excessive duration of this study. I am grateful to Dr. Helen E. Grenga and Dr. Edgar A. Starke, Jr. for their comments and cooperation in reviewing this work.

I sincerely appreciate the help and comments of Dr. Miroslav Marek, regarding the electrochemical portion of this study. My thanks are extended to Mr. Charles R. Blackwood and Mr. Joe Kilpatrick for their help in the preparation of specimens. I thank Mr. Larry H. Glassman for his cooperation and comments.

I gratefully acknowledge the support of the National Institute of Dental Research, the Texaco Corporation, and ARPA Order 878.

I wish to thank my family for patience, trust, and cooperation during this lengthly project. I am grateful to all my friends in the Department of Chemical Engineering and Metallurgy for their advice, discussions, and good cheer throughout my graduate study.

TABLE OF CONTENTS

LIST OF TABLES

LIST OF FIGURES

LIST OF FIGURES (Continued)

SUMMARY

Hydrogen induced delayed failure characteristics were investigated for AISI 4340 steel quenched and tempered to the 260 to 280 ksi strength level, coated with a porous cadmium electroplate, and immersed in aqueous 3.5 per cent sodium chloride. Notched specimens were stressed in constant moment cantilever bending. Opening mode stress intensity was used to quantify the stressing conditions, and time to failure was determined for a wide range of initial stress intensities.

Fracture surfaces were analyzed by scanning electron microscopy. The fracture mode for hydrogen embrittlement under plane strain deformation conditions was found to be mixed intergranular separation and quasi-cleavage.

The electrochemical behavior of the 4340 steel - cadmium couple in aqueous 3.5 per cent sodium chloride was investigated. Measurements of direct coupling current and open-circuit potential difference were made, and single electrode studies of potentiodynamic polarization and free corroding potential were also carried out. It was determined that cadmium is continuously anodic to 4340 steel for times of interest to the delayed failure problem.

Scanning electron microscopy and light optical microscopy were used to examine the nature of the cadmium electrodeposit before and after hydrogen relief baking at 395°F. The electrodeposit was found to consist of clusters of small platelets. The baking treatment apparently caused an agglomeration of the cadmium clusters, resulting in a signifi-

cant increase in the porosity of the plating.

Electrochemical studies indicated that conditions are favorable for hydrogen evolution on exposed steel at the bottom of pores in the plating; therefore, it is probable that the sacrificial corrosion of the cadmium electroplate promotes hydrogen embrittlement. In delayed failure testing, baked specimens exhibited significantly shorter times to failure than as-plated specimens. This decrease in the time to failure was attributed to increased hydrogen availability resulting from the noted increase in exposed steel area caused by the baking treatment.

CHAPTER I

INTRODUCTION

The presence of hydrogen in metals and the attendant problems have been studied for more than a century, but interest in the subject has greatly intensified in the past three decades. The deleterious effect on the mechanical properties of high strength martensitic steels caused by extremely small amounts of hydrogen is one of the most striking aspects of the problem. This phenomenon is most commonly referred to as "hydrogen embrittlement" (HE). In other forms of "embrittlement" increasing strain rates and decreasing temperatures accentuate the brittle behavior; just the opposite is true for HE, in fact, the worst known conditions are static load and room temperature. The term "hydrogen induced delayed failure" has been used to refer specifically to HE under static loading conditions.

In recent years there has been an increasing quest for higher strength materials, and low alloy martensitic steels such as AISI 4340 have been among the most promising. However, the occurrence of hydrogen induced failures under static loads far below the yield stress and an apparent increase in hydrogen embrittlement susceptibility with increasing strength level have hindered full utilization of the outstanding mechanical properties of such steels.

Many of the structures in which service failures have been experienced were electroplated with cadmium. The introduction of hydrogen

into the steel during pickling and plating processes has long been recognized as dangerous. Much effort has been devoted to reduction of hydrogen embrittlement problems associated with cadmium plating processes. The avowed purpose for plating these steels is the prevention of corrosion, and the porous cadmium plating used in this study has been widely accepted as a means of obtaining corrosion protection with minimum danger of HE resulting from hydrogen introduced by plating.

The corrosion protection of steel by cadmium plating is based on sacrificial corrosion of the cadmium. The cathodic polarization of steel by this process could result in hydrogen entering the steel. In view of the susceptibility of high strength martensitic steels to embrittlement by extremely small amounts of hydrogen, sacrificial corrosion of cadmium plating could cause hydrogen embrittlement. Electrochemical studies were undertaken in order to evaluate the possibility of HE resulting in this manner.

In spite of the vast amount of literature on hydrogen embrittlement, there is little data directly concerning the effects of galvanic corrosion. A major intent of this study was to supplement the literature in this area, in hopes of promoting a more circumspect approach to the hydrogen embrittlement problem.

CHAPTER II

REVIEW OF THE LITERATURE

The amount of literature pertaining to the problems caused by hydrogen in steels is enormous. Several detailed reviews are available (1-7), varying in scope and purpose,and the present review is intended only to provide a background for the experimental work to be subsequently presented.

Models for Hydrogen Cracking

Since no model for the mechanism of hydrogen embrittlement has been generally accepted, a brief discussion of the various proposed models will be presented, with emphasis on their application to delayed failure of high strength steels. There has been much controversy, and some confusion as well, associated with the theoretical aspects of hydrogen embrittlement; however, this should be viewed with an appreciation for the complexity of the problem and the proliferation of its research. Dozens of parameters have been studied by hundreds of investigators, resulting in thousands of publications.

The proposed models may be divided into four categories, which will be presented in chronological order of their initial appearance.

Pressure Model

Zapffe and his co-workers (1,8) were the first to attempt a theoretical explanation of hydrogen embrittlement. Their model, called the planar pressure theory, was based on a "block"or "mosaic" concept of

metallic structure. It was proposed that atomic hydrogen enters the lattice until extreme supersaturation, then in an ageing type phenomenon it precipitates at block boundaries, where hydrogen gas is formed. Enormous pressures are said to be built up before equilibrium is reached. The stresses due to this internal pressure would be additive to externally applied stress, thereby lowering the apparent fracture stress. Although this concept was originally only intended to explain transcrystalline cracking in pure iron, it was later extended to other cases.

With advancements in fundamental metallurgical knowledge, various investigators (9-15) have proposed modifications of the planar pressure theory. DeKazinczy (10) suggested that the sites of precipitation are Griffith flaws or similar cracks, and he calculated the energy contribution of adiabatic expansion of occluded hydrogen gas during extension of a Griffith crack. Bastien and co-workers (9) proposed that hydrogen is condensed around dislocations and during fracture this hydrogen is discharged into the active crack, tending to maintain high pressure. Others (12,15) suggested that the crack initiation sites are wedge-shaped micro-cracks, and some calculations were presented for the extension of these cracks by the combined action of internal pressure and external stress.

Adsorption Models

Petch and Stables (16) were the first to advance a theory for hydrogen embrittlement which accounted for the time delay aspect observed in hydrogenated high strength steels under static load. Their model was adapted from the brittle fracture theories for glass developed by Griffith and Orowan. The cracking process is assumed to start at a pre-existing

Griffith flaw, which will extend under an applied stress above some critical limit. In the absence of hydrogen, it is proposed that the crack would quickly stop due to the high energy of the newly formed surface. However, if hydrogen is present, it is presumed to migrate to this new surface and become adsorbed, thereby lowering the energy of the surface so that the crack may extend again. This cycle of events would be repeated until the crack is so large that the remaining section is overstressed, then complete fracture would occur. After further research, Petch (17) described his theory in greater detail and presented some calculations of the magnitude of reduction in fracture stress, based on his model.

Lattice Embrittlement Model

In the course of extensive investigations of hydrogen induced delayed failure, Troiano and co-workers (18-23) developed a model in which the hydrogen dissolved in the lattice lowers the true cohesive strength of the metal. Hydrogen is presumed to concentrate in the region of highest triaxial stress as a result of stress induced diffusion, until a critical combination of stress and hydrogen concentration is reached. Then a crack is initiated which propagates until it leaves the hydrogen rich zone; whereupon, stress induced diffusion concentrates hydrogen in the region of maximum triaxial stress ahead of the stopped crack and the process is repeated until the load cannot be sustained by the remaining section, and total failure occurs. Like the adsorption model, this mechanism provides an explanation of the discontinuous nature of hydrogen induced delayed failure in high strength steels.

The low temperature plastic straining and ageing experiments of

Morlet et al. (19) indicated that the damaging species is lattice dissolved hydrogen. Johnson et al. (20) working with uniformly hydrogenated notched stress-rupture specimens, demonstrated the existence of an "incubation" period during which no permanent damage occurs. The establishment of a critical hydrogen concentration by stress induced diffusion was presumed to be responsible for this period, since it was found to be reversible with respect to stress. The crack initiation was shown to be subsurface, and depth varied with notch acuity in the same manner as the region of maximum triaxial stress.

Hydrogen Assisted Deformation Model

Recently, Beachem (7) has proposed a model in which lattice dissolved hydrogen concentrates in regions of high triaxial stress and "aids whatever deformation processes the microstructure will permit." The observation that all hydrogen failures examined by electron fractography show evidence of microscopic plasticity led to the conclusion that hydrogen induced delayed failure is not a form of embrittlement, and that the term "hydrogen assisted cracking" (HAC) would be more appropriate than the term "hydrogen embrittlement".

In electron fractography of wedge-open loaded (WOL) specimens, Beachem found the first stage of cracking to be by microvoid coalescence (MVC). A general decrease in the extent of plasticity of the fracture mode with decreasing stress intensity was also observed. In view of the fact that the plastic zone size is proportional to the square of the stress intensity, it was postulated that this relation for fracture surface plasticity probably is a general rule.

The Influence of Cadmium Electroplating

Cadmium electroplating is known to be a common cause of hydrogen embrittlement in high-strength steels. Available data from the literature centers around the introduction of hydrogen during plating and its removal by a subsequent thermal treatment, usually referred to as baking.

One frequently discussed parameter, current efficiency, is an expression of the percentage of plating current which deposits metal on the cathode. In aqueous plating baths, the remaining percentage of the current is presumed to deposit hydrogen (24-27). But the conditions of hydrogen absorption during plating are much more complex than this, as evidenced by the following observations:

(1) delayed failure suffered by specimens plated at approximately 100 percent current efficiency (27).

(2) absorption of a damaging quantity of hydrogen required less time for Cd plating at 90 percent current efficiency that for pure hydrogen plating (24).

The baking treatment for removal of hydrogen was extensively studied by Brown (25) and found not to be an absolute preventive for delayed failure. Since the diffusion rate of hydrogen through cadmium is lower than that through steel, several investigators have considered it probable that hydrogen is sealed in by a continuous cadmium layer, and under these conditions the effect of baking is mainly a redistribution of the initially subsurface hydrogen throughout the steel (20,25, 27,28). It is generally accepted that porous cadmium plating reduces the problem of hydrogen cracking by facilitating the removal of hydrogen during baking (25-28), but the coating must also be sufficiently thick

and adherent to serve its primary purpose of providing corrosion protection.

Electrochemical Implications

Various investigators have recognized the fact that cadmium is generally anodic to iron and steel (27-29), and sacrificial protection has been attributed to cadmium plating of steels (27,28,30). Cash and Scheuerman (28) performed salt spray corrosion experiments independent of delayed failure testing, and Geyer et al. (27) tested some steel specimens with a vacuum metallized cadmium coating under sustained load before and after salt spray corrosion tests, but no testing was done which combined sustained load and corrosive exposure. Read (31) briefly discussed the possibility that cracking could be caused by hydrogen from a corrosion process, but he dismissed it as a rare problem and one that had not been associated with metal finishing. Peterson, et al. (32) suggested that cathodic protection of high-strength steels in sea water might not be beneficial in view of the problem of hydrogen embrittlement. They further found that coupling a high-strength maraging steel to zinc in NaCl promoted stress corrosion cracking. Electrochemical reactions on 4340 steel in NaCl solutions were intensively studied by Toy (33). He used polarization curves to characterize the effects of stress, pH, heat treatment, and oxygen content of the solutions. Zanker and Yahalom (29) studied the free corroding potentials and galvanic coupling of pure iron and cadmium in dilute NaCl solutions and found cadmium to be continuously anodic to iron.

CHAPTER III

EXPERIMENTAL PROCEDURE

Materials and Specimen Preparation

All the specimens for this work were cut from a single piece of aircraft quality E-1 4340 (MIL-S-5000C), one-half inch plate. The analysis of this steel is shown in Table 1.

Table 1. Alloy Composition

Element	C	Mn	Si	Cr	Ni
Weight Percent	0.410	0.62	0.24	0.77	1.83

Element	Mo	P	S	Fe
Weight Percent	0.22	0.032	0.029	Balance

Specimens for Delayed Failure Testing

Specimens were designed for delayed failure (DF) testing in a constant moment cantilever beam bending apparatus, as described by Brown (34). The dimensions of these specimens are shown in Figure 1a. The longitudinal axis of the specimens was in the rolling direction and the cracking direction was the long transverse. This crack propagation system has been designated RW (35). Rough dimensions were produced by milling and final dimensions by surface grinding. The notches were

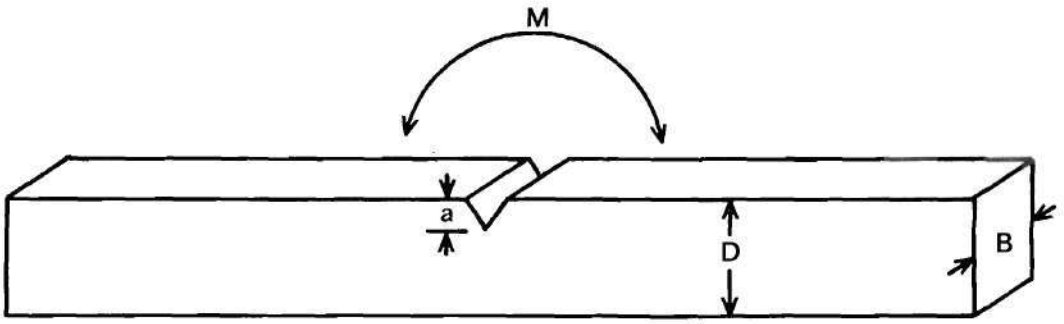

D = 5/8 inch
B = 1/2 inch
a = 1/8 inch

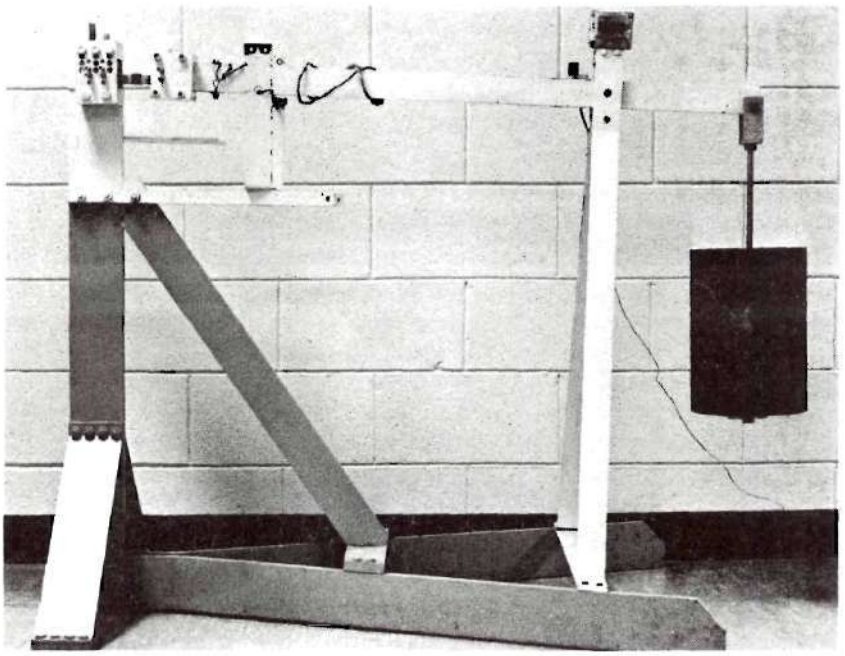

Figure 1. (a) Delayed Failure Specimen and Dimensions. (b) Cantilever Bending Apparatus.

milled to produce a flank angle of sixty degrees and a root radius of seven to eight mils. Light finishing cuts were made using a shaper with a carefully prepared tool of tip radius 0.005 inch. Final notch finishing was done with a hand operated wire saw using annealed 302 stainless steel wires and water mixed alumina abrasives. The root radius of the notch was reduced to 0.004 inch using twenty micron alumina and final finishing was done with three micron alumina. This procedure produced very uniform notches with a fine surface finish.

Heat treating was done after all machining and grinding operations were completed. Austenitizing was done at 1550°F in a controlled atmosphere to minimize the possibility of surface decarburization or carburization. Subsequent microhardness measurements at varying depths using an angle ground test piece indicated that the furnace atmosphere control had been satisfactory. The specimens were quenched in well agitated oil. Care was taken to minimize the time from furnace to quench. Tempering was done at 400°F to attain a tensile strength of approximately 275 ksi, estimated from hardness measurements.

After heat treatment some specimens were set aside for determination of K_x, while the remainder were electroplated. Some of the plated specimens were baked for 23 hours at 395°F (202°C) immediately following the plating operation; the others were to be tested as-plated.

Specimens for Electrochemical Studies

Specimens for polarization and coupling studies were cut from a cast rod of pure cadmium (Baker 100.0 weight percent assay) 0.36 inch in diameter and from the shank of a delayed failure specimen ground to the same diameter. A plated and baked sample 0.25 by 0.50 inch was also

prepared, for determination of free corroding potential versus time. All surfaces not of interest were masked with epoxy to prevent reactions and to minimize edge effects.

Testing Solution

An aqueous, 3.5 weight per cent sodium chloride solution was used for delayed failure tests and electrochemical studies. All solutions were prepared from U.S.P. grade, granular NaCl and distilled water. In all tests the solutions were discarded after use.

Electroplating

Specimens were dry abrasive blasted just prior to plating, rinsed with tap water and brushed to remove abrasive particles, dipped in a solution of NaCN, and immediately immersed in the plating bath. The composition limits of the plating bath are given in Table 2. Current density was 60 amperes per square foot and the current was applied immediately after immersion of the specimens. Plating time was approximately five minutes, with the resulting porous cadmium layer being about 0.0005 inch thick. Immediately after plating, the specimens were rinsed with tap water, dipped in a dilute solution of chromic acid, then rinsed and dried.

Delayed Failure Testing

Equipment

Figure 1b shows the cantilever beam testing apparatus, with a specimen in place. The time to failure was measured by an electric timer with a microswitch contacting the side of the loading beam, so that only complete rupture of a specimen would stop the timer. The span

Table 2. Plating Solution Composition Limits

Cd (in the form of CdO)	2.9 - 5.5 oz/gal.
Na_2CO_3	2.0 - 8.0 oz/gal.
NaCN	12.0 - 20.0 oz/gal.
NaCN: CdO Ratio	2.8 - 6.0
NaOH (free)	1.0 - 3.2 oz/gal.
pH	above 12
temperature	70° - 90°F

between the grips was 2.5 inches, with the notch in the center of the span. A gear-reduction scissors jack was used to lower the load bucket, in order to minimize loading shock. For one test an acoustic emission transducer was fastened to the shank of a delayed failure specimen. The transducer output was amplified and recorded on a strip chart.

Experimental Procedure

The loading program for delayed failure testing was based on an experimental value of the stress intensity for failure on rising load in air, which shall be referred to as K_x. An unplated specimen was used for this test. Plated specimens to be tested in the NaCl solution were fitted with polyethylene cups attached around the notch with Silastic cement. Several days ageing time was allowed for the Silastic to cure and release all acetic acid. In all cases the load was applied before the solution was added; timing was begun upon introduction of the solution. Some of the plated specimens to be tested in air were also fitted with corrodant vessels.

Fractography and Metallography

Scanning electron fractography, performed on a Cambridge Stereoscan, was used extensively for analysis of the cracking process. Fresh fracture surfaces were thoroughly rinsed to remove the testing solution, dried, coated with a light grease, and stored in a dessicator. Sectioning for fractography and metallography was done with an abrasive cutoff wheel, and the protective layer of grease was not removed until after sectioning. The fracture surfaces were rinsed with trichlorethylene to remove the protective grease and immediately rinsed with ethanol in order to leave the surface free of residue. Samples of the plated

surface were also sectioned for SEM and metallographic examination. A tilt angle of 30 degrees was used for all SEM work. Metallographic sections perpendicular to the fracture surface and sections perpendicular to the plated surface were prepared from selected delayed failure specimens. Light optical micrographs were taken on a Vicker's Model 55 Metallograph.

Electrochemical Studies

Polarization Experiments

Polarization curves for steel and cadmium were determined potentiodynamically, using the electrolytic cell shown in Figure 2a. The cell is essentially a glass beaker with a flat flange at the top and a glass lid ground to fit. There are taper ground joints in the side of the cell to accommodate the specimen and a platinum counter electrode. The lid is held in place by spring clips and has ground joints to accept a salt bridge type remote reference junction and a gas tube for dearation of the solution. A copper wire was attached to the sample with silver cement for electrical connection to the potentiostat. A glass tube was placed around the wire, then the sample and tube were encased in epoxy. The specimen design is shown in Figure 2b. The specimen surfaces were freshly ground through 600 grit wet abrasive paper immediately before immersion.

The potentiostat used was a Wenking Model 68TS3. A Hewlett-Packard Model 7001AM X-Y recorder was used to plot the output in standard polarization curve form. The testing solution was dearated with dry nitrogen for 30 minutes prior to the start of each run. During this time the equipment was allowed to warm up. The cathodic scan for the

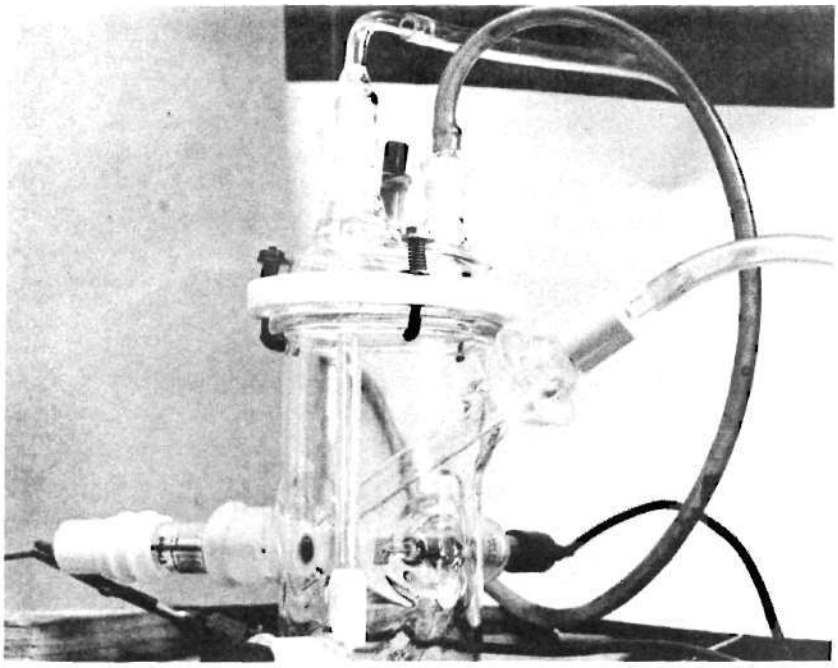

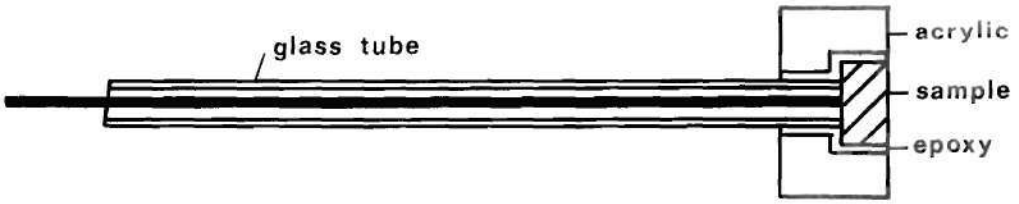

Figure 2. Potentiodynamic Polarization Apparatus: (a) Electrolytic Cell; (b) Specimen Design.

steel was begun at approximately 0.7 volts versus saturated calomel electrode; two minutes after the termination of the cathodic scan, the anodic scan was begun. The anodic scan for cadmium was started at approximately -1.6 volts SCE. The applied potential was stepped in two millivolt increments at the rate of 10 steps per minute. Polarization curves for the steel and cadmium in aerated NaCl solution were obtained in the same manner.

Free Corroding Potential

Free corroding potential versus time for steel, cadmium, and cadmium plated steel in the NaCl solution was studied using a Keithley Model 602 millivolt electrometer. Specimens were prepared in the same manner as for polarization studies, with everything except the surface of interest sealed with epoxy. The steel and cadmium specimens were wet ground through 600 grit immediately prior to testing. Potential was measured with respect to a saturated calomel electrode. The tip of the calomel electrode was placed a short distance away from the specimen surface to give a reliable average potential.

Coupling

The behavior of the cadmium-steel couple in the NaCl testing solution was studied by measurement of the open circuit potential difference and the short circuit current. The Keithley 602 electrometer was used to measure potential and the data was recorded manually. For current versus time studies the electrometer was used in conjunction with a Honeywell Electronik 193 strip chart recorder. The samples prepared for polarization were freshly reground and placed in the testing solution with their surfaces coplanar and their nearest edges about 1 cm apart.

CHAPTER IV

RESULTS

Delayed Failure

The stress intensity for failure on rising load in air gives a reasonable measure of the maximum loading condition the specimen design will permit. This value, which is called K_x, was determined to be 115 ksi $\sqrt{in}$. The relation

$$K_I = 4.12\ M(\alpha^{-3} - \alpha^{3})^{\frac{1}{2}}/BD^{3/2} \qquad (34)$$

was used to calculate opening mode stress intensity; where M is the bending moment in inch-pounds, B, D, and a are the specimen thickness, height and crack depth, respectively, and α is $1 - \frac{a}{D}$. The choice of load for each of the delayed failure tests was based on K_x. The results of the delayed failure testing are summarized in figure 3. The baked specimens tested in air sustained high loads for long periods of time, and could thus be judged immune to delayed failure in air under normal working stresses. Both baked and unbaked sets of samples tested in the NaCl solution exhibited typical hydrogen induced delayed failure behavior. Upper critical stress intensities were slightly below K_x. The lower critical stress intensities were within the range of normal service conditions for high strength parts containing stress raisers. A large portion of the range between the upper and lower limits was quite insensitive to differences in stress intensity. In this range acoustical monitoring was used to separate the incubation period from the crack

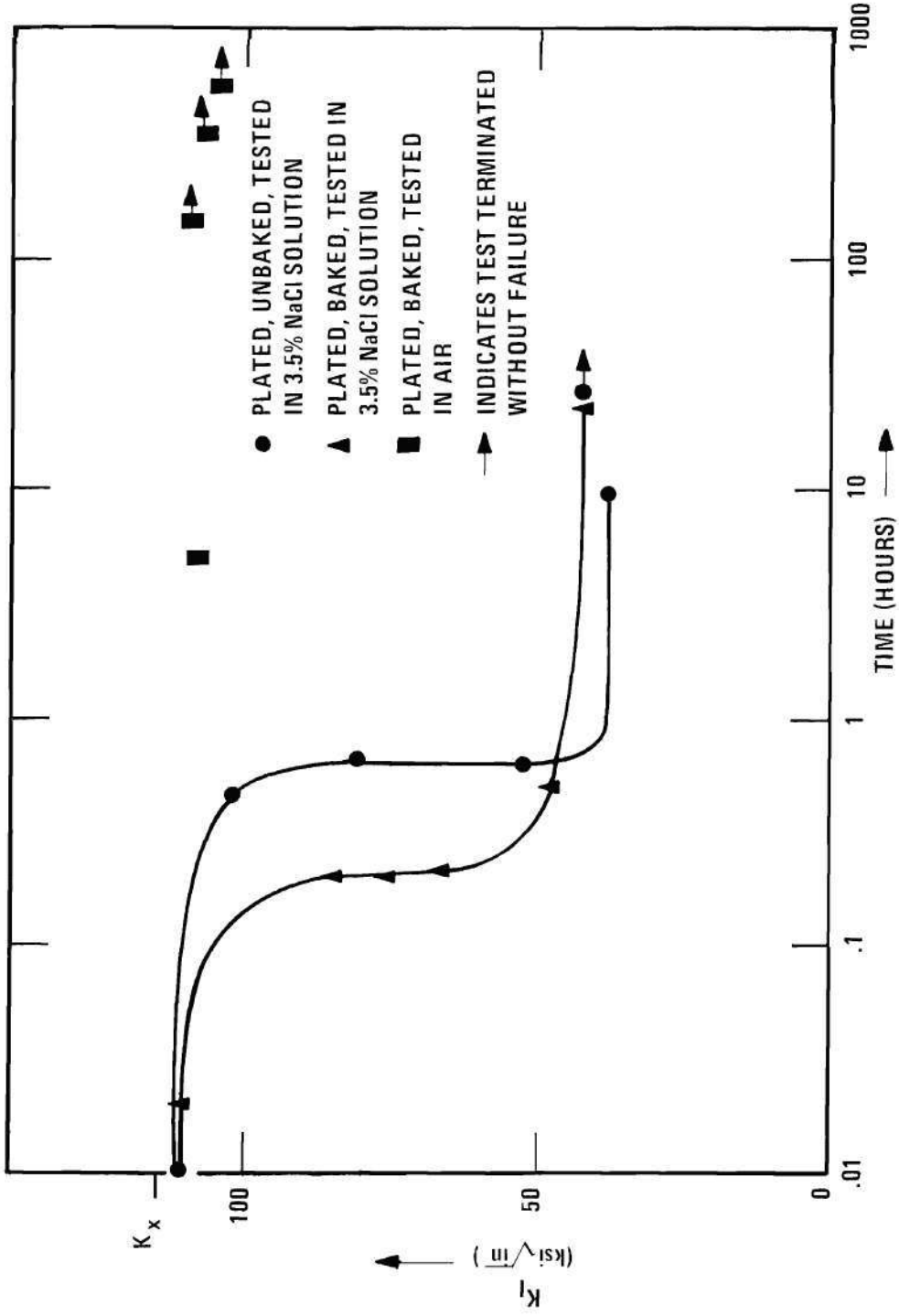

Figure 3. Influence of Baking on Delayed Failure Characteristics.

propagation time. Audible "clicking" was noted for a period of about one to three minutes prior to failure. Acoustic emission detection equipment was used in one test and the reliability of observations by the unaided ear was confirmed in that the amplitude of the initial "click" was on the order of the maximum amplitude recorded. The incubation period for the unbaked specimens was found to be about three times that of the baked specimens.

Fractography

The macroscopic appearance of the fracture surfaces is illustrated in figure 4. Measurements from the macrograph of the K_x sample showed that the total width of the shearlips was about 14 percent of the specimen thickness. According to Tetelman and McEvily (36), this indicates that the deformation conditions were 86 percent plane strain. Theoretical estimates of shearlip width were made, based on a relation for the plastic zone size (r) at the free surfaces of a through thickness crack

$$r = \frac{K_I^2}{2\pi \sigma_{ys}^2} \qquad (37)$$

where K_I is opening mode stress intensity and σ_{ys} is yield strength. Using the K_x value and a yield strength of 240 ksi estimated from hardness measurements, the calculated shearlip width was in agreement with the measured value. For delayed failure specimens, a macroscopically rough region of apparent slow crack growth by hydrogen embrittlement could be readily distinguished from the flat areas of fast fracture, as seen in figure 4b. Shearlips were present in all delayed failure speci-

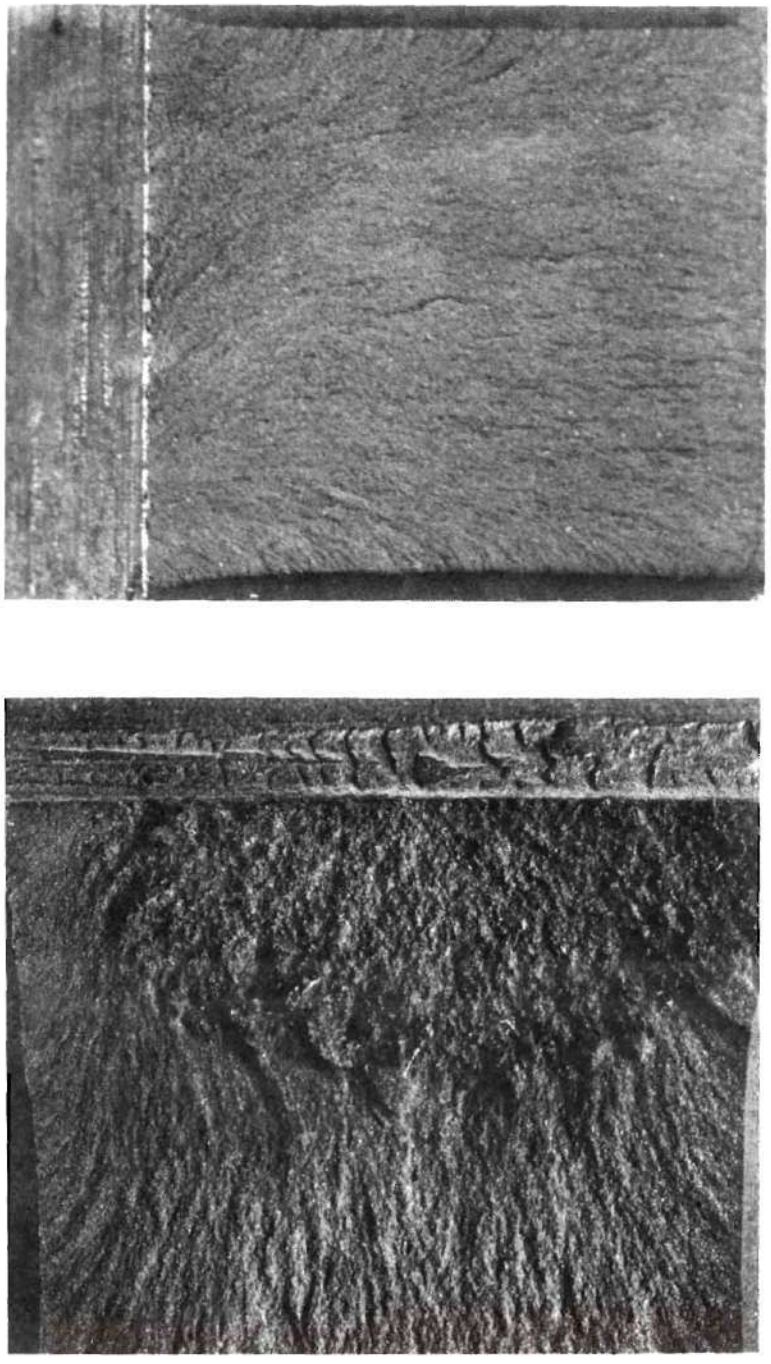

Figure 4. Macroscopic Appearance of Fracture Surfaces: (a) K_x Specimen; (b) Typical Hydrogen Embrittlement Fracture.

mens; however, they were much smaller adjacent to slow crack growth areas, as has been noted previously (38,39).

Five samples, representing a wide range of initial stress intensities in both the baked and as-plated conditions, were chosen for scanning electron fractography. This technique provides the high magnification and great depth of field necessary for investigating fine scale fracture features. In all cases the macroscopically apparent slow crack growth zone exhibited mixed fracture modes. The predominant modes were found to be intergranular separation (IG) and quasi-cleavage (QC); examples are shown in figure 5. The IG cracking apparently followed prior austenite grain boundaries, while many isolated grains were cut through by QC. No large regions of QC were found. Some small patches of micro-void coalescence (MVC) were seen throughout the slow crack propagation region, and they were somewhat more numerous near the transition to fast fracture. Figure 6 shows an MVC (ductile fracture) region adjacent to the notch root; it consisted almost entirely of equiaxed dimples. The presence of this region indicates that hydrogen embrittlement crack initiation was subsurface, as was reported by Johnson, et al. (20).

Examination of the Electrodeposit

Quite in contrast to conventional bright cadmium plating, the porous deposit was light gray in color and had very little luster. Great care had to be taken in the preparation of metallographic specimens in order to prevent damage to the cadmium. Extremely flat surfaces had to be maintained for high magnification examination of the cross sections of the electrodeposit. It can be readily seen in figure 7

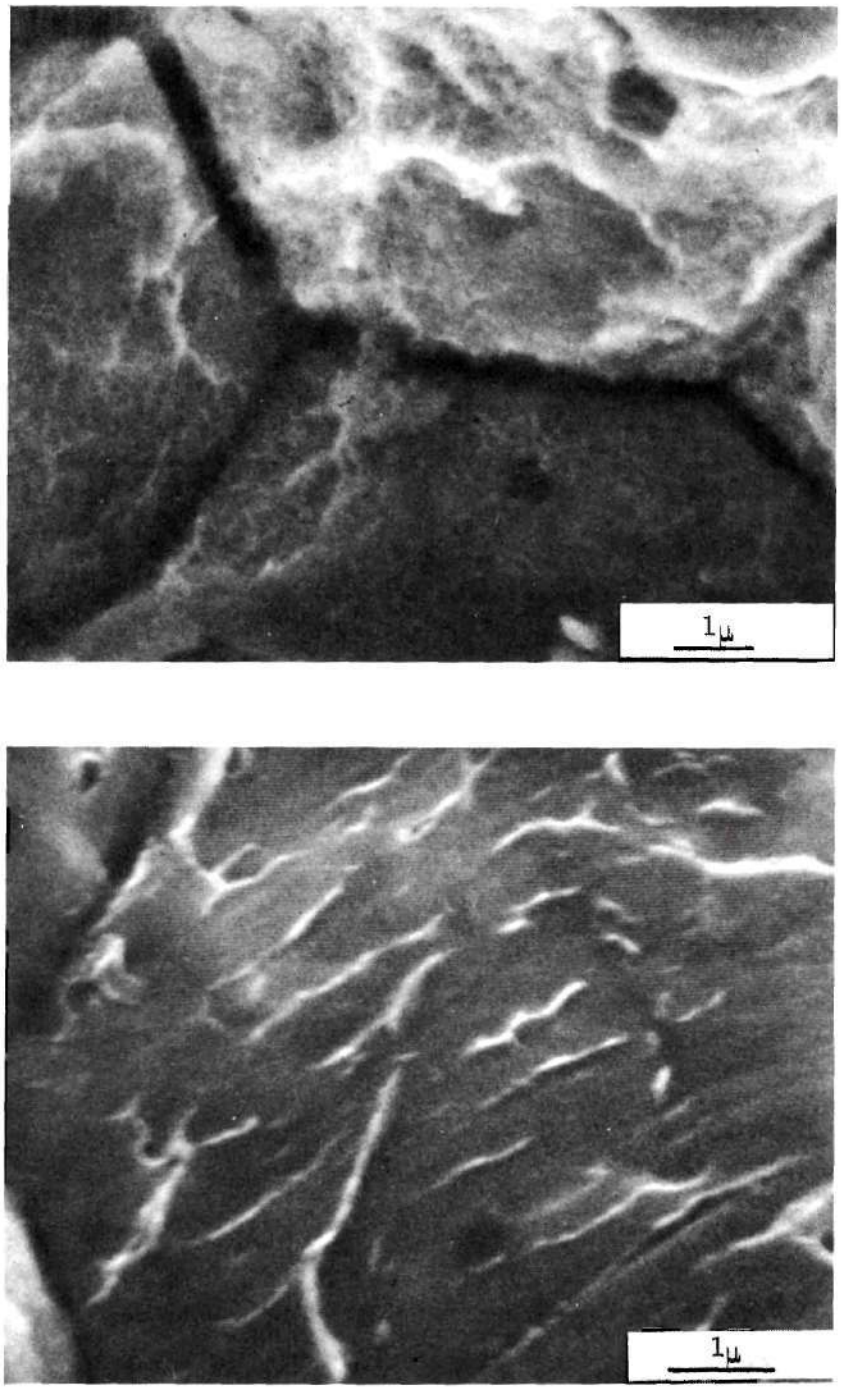

Figure 5. Scanning Electron Micrographs of Hydrogen Embrittlement Fracture Modes: (a) Intergranular Separation Along Prior Austenite Grain Boundaries; (b) a Quasi-Cleavage Facet.

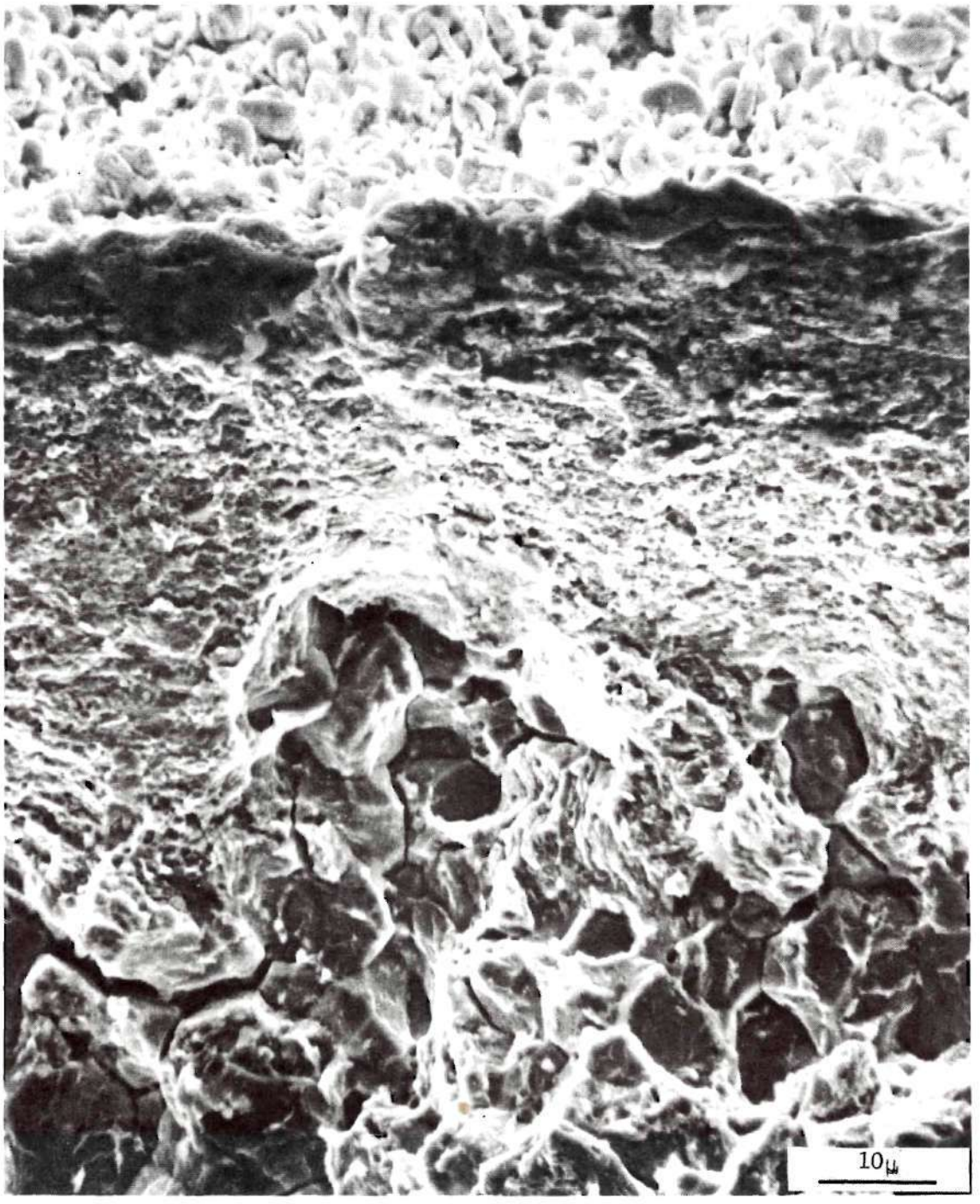

Figure 6. Scanning Electron Fractograph of the Crack Initiation Region. Plating at the Notch Root, Simple Rupture Region Adjacent to the Notch Root, and the Initiation of Hydrogen Embrittlement Fracture, Top to Bottom, Respectively.

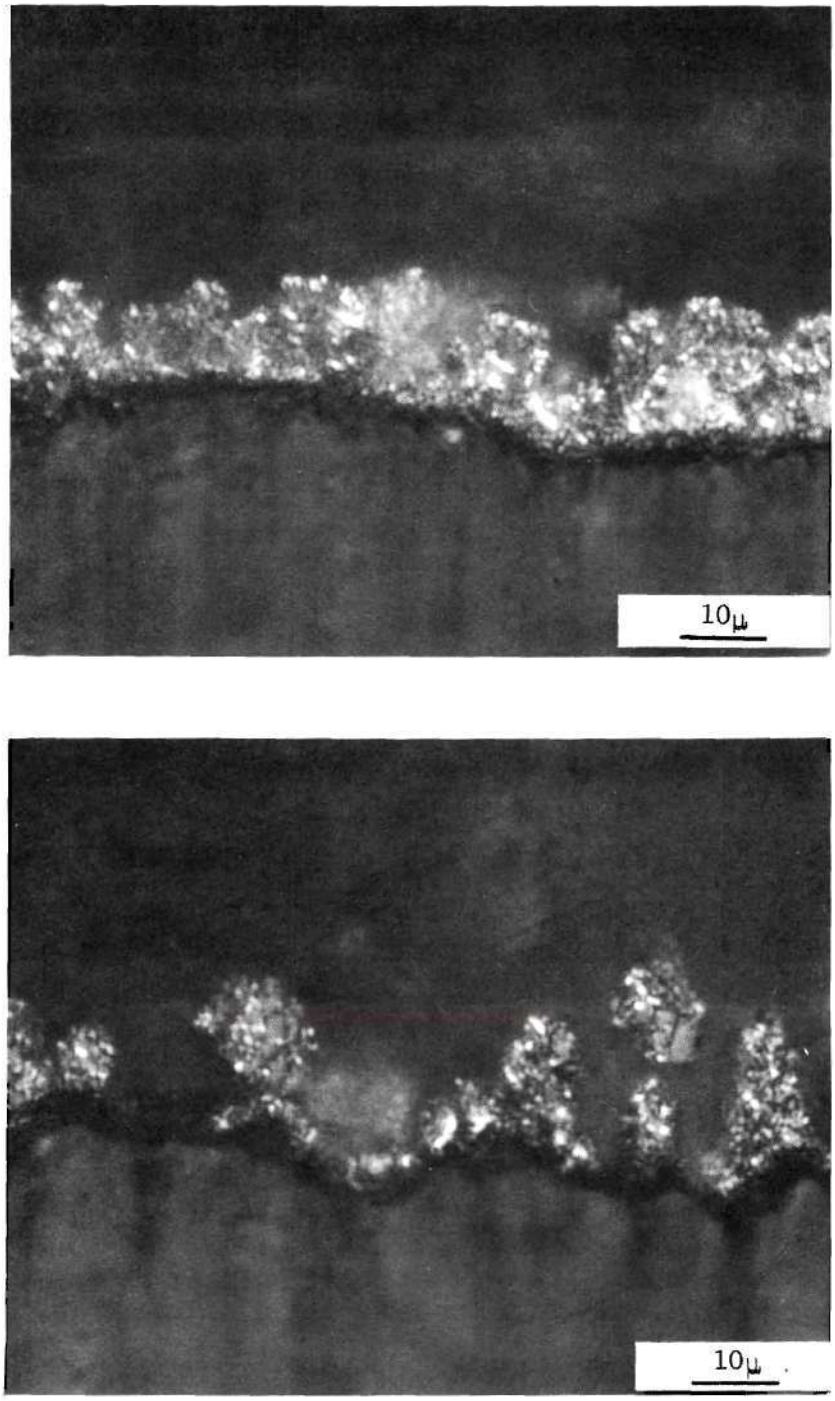

Figure 7. Polarized Light Micrographs of Cross Sections of the Cadmium Plating: (a) As Plated; (b) Baked 23 Hours at 395°F.

that the baking treatment has altered the plating, increasing its height by about one third and greatly increasing its porosity. Examination of similar samples by SEM revealed that the deposit consists of clusters of platelets, as seen in figure 8. Some rather large pores were found in the case of the baked sample.

Electrochemical Studies

The results of the potentiodynamic polarization experiments are summarized in figures 9 and 10. The data from the linear x-y charts of current versus potential was transposed to log current density versus potential. For the steel in deaerated NaCl, both cathodic and anodic curves were made for comparison with data Toy (33) obtained under fairly similar conditions; the agreement was reasonable and consistent. Since the central interest of this study was the sacrificial protection of the steel by cadmium, only the anodic branch of the polarization curves for cadmium and the cathodic branch for steel in aerated NaCl were determined. It was found that cadmium is anodic to the steel in the test solution.

The free corroding potentials for the steel, cadmium, and cadmium plated steel in the NaCl solution open to the air were found to vary with time as shown in figure 11. Cadmium was significantly electronegative to the steel throughout a 1000 minute testing period. The potential of the steel fell erratically in the early stages of the experiment, then became fairly stable at a value between -0.60 and -0.62 volts SCE. The potential of the cadmium was stable for a long period of time, but then it shifted about 0.07 volt electropositively (beginning its rise at test times between 400 and 2500 minutes) presumably due to film formation. The potential of plated samples (baked and as-plated) was

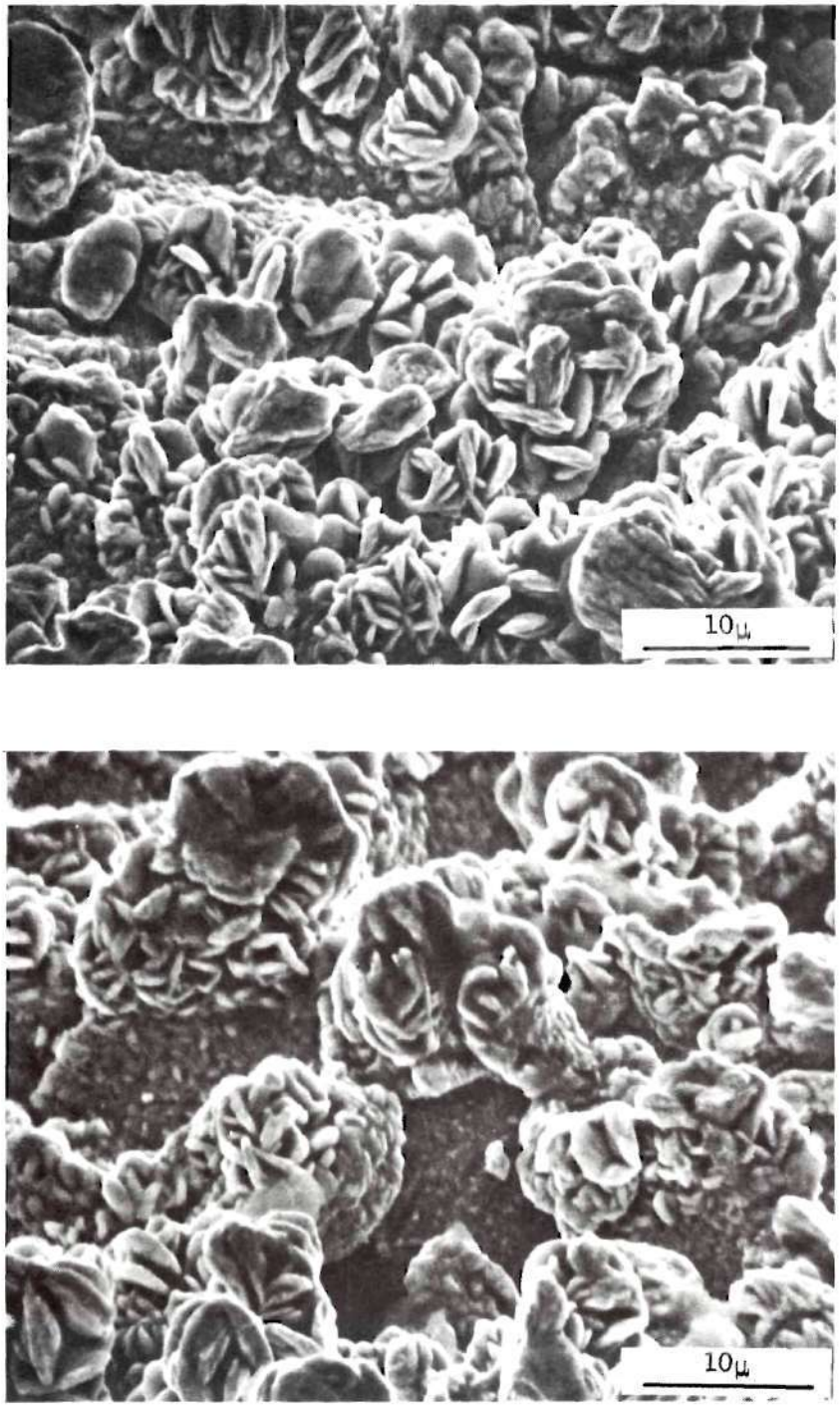

Figure 8. Scanning Electron Micrographs of the Cadmium Plating: (a) As Plated; (b) Baked 23 Hours at 395°F.

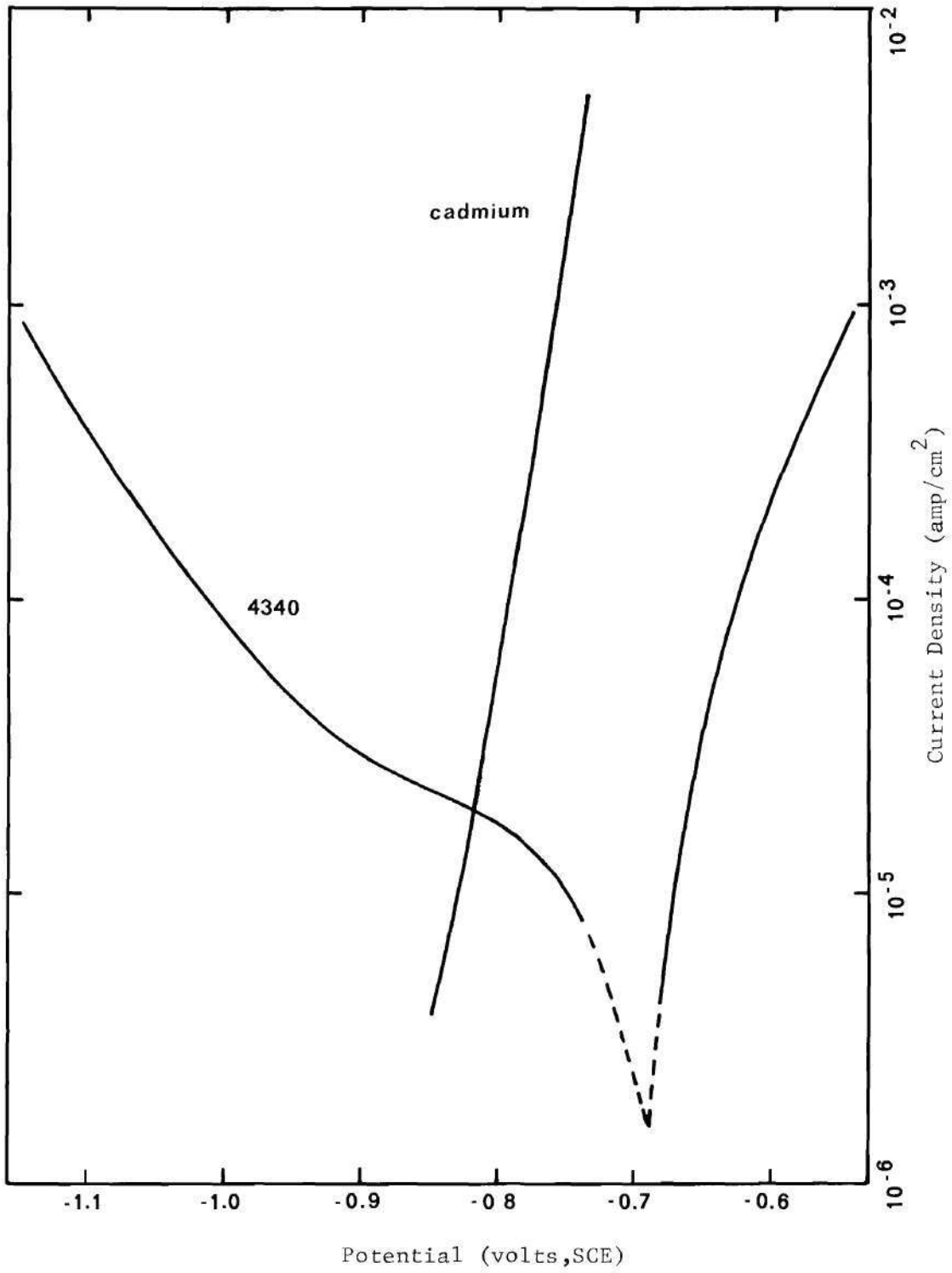

Figure 9. Potentiodynamic Polarization Curves in Deaerated 3.5 per cent NaCl.

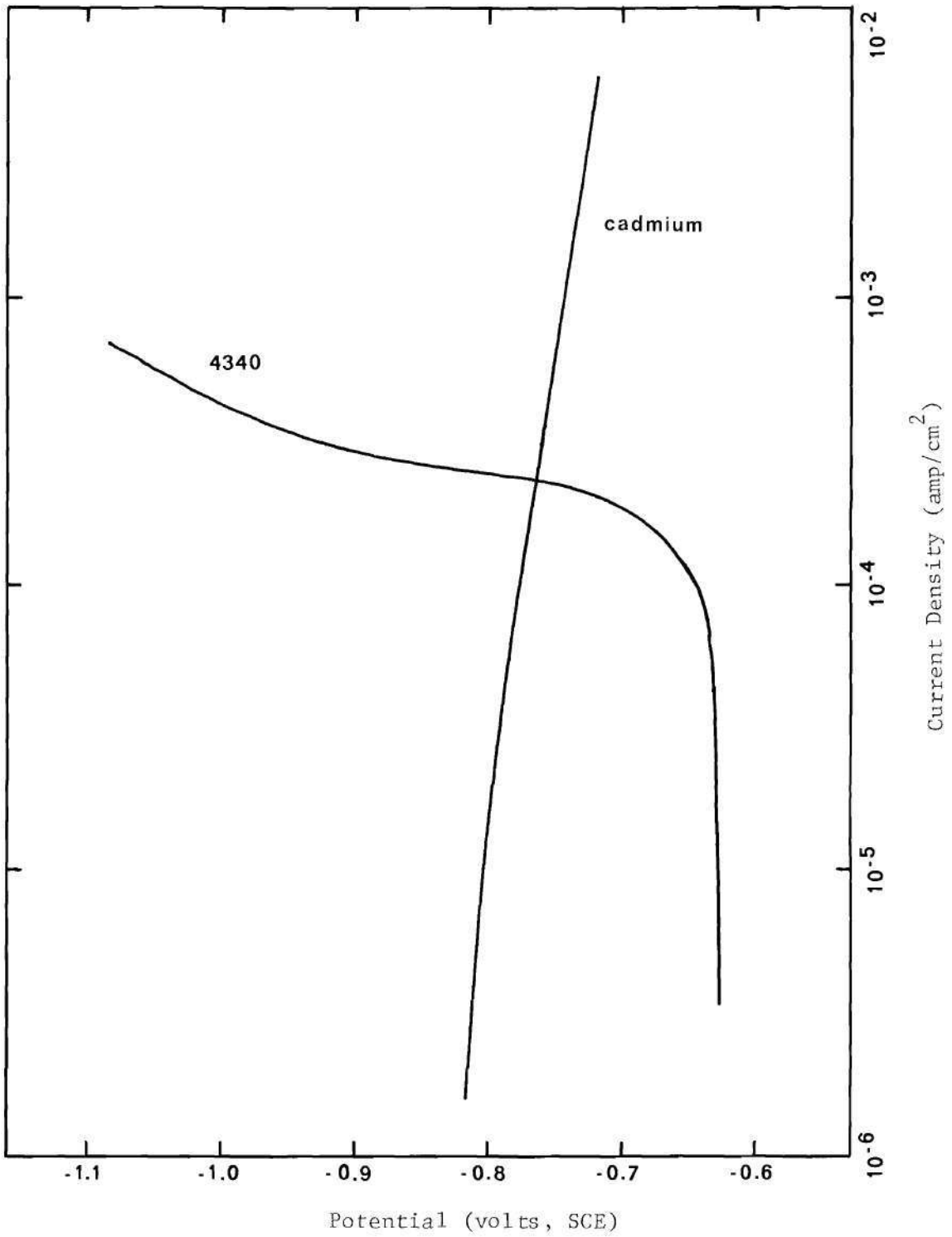

Figure 10. Potentiodynamic Polarization Curves in Aerated 3.5 per cent NaCl.

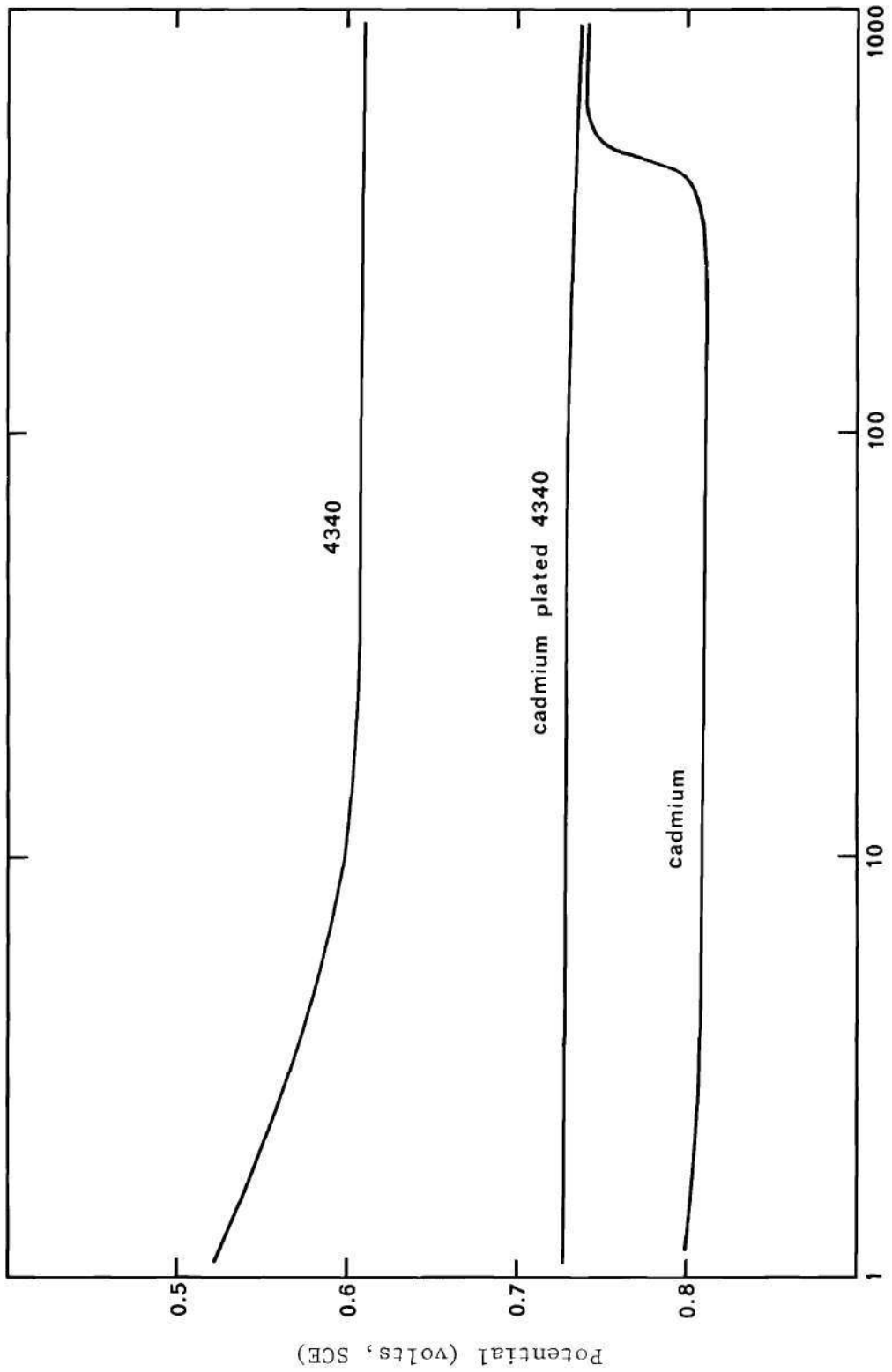

Figure 11. Free Corroding Potential Behavior in 3.5 per cent NaCl, Open to the Air.

stable throughout the 1000 minute test period; however, when samples were left in the solution for several days a film formed which eventually covered the surface of the plating, then sacrificial protection ceased and the potential shifted close to the value for corroding steel. Samples of the steel and cadmium were also tested after being ground, dried, and stored in a dessicator for one week. Both samples exhibited potentials which were initially electropositive with respect to their freshly ground counterparts, but these differences dropped to zero in less than 100 minutes.

Although the single electrode studies indicated that cadmium is continuously anodic to the steel for times much greater than the incubation period for delayed failure, equal area coupling experiments were considered necessary for a more complete understanding of the steel-cadmium cell. Measurements of direct coupling current versus time and open circuit potential difference versus time were made. The results of these experiments are presented in figure 12. The current density initially dropped very rapidly, but after about 15 minutes it became reasonably steady at about 20 $\frac{\mu \text{ amp}}{\text{cm}^2}$. The potential difference (cadmium anodic) became quasi-steady at a value slightly greater than 0.25 volt.

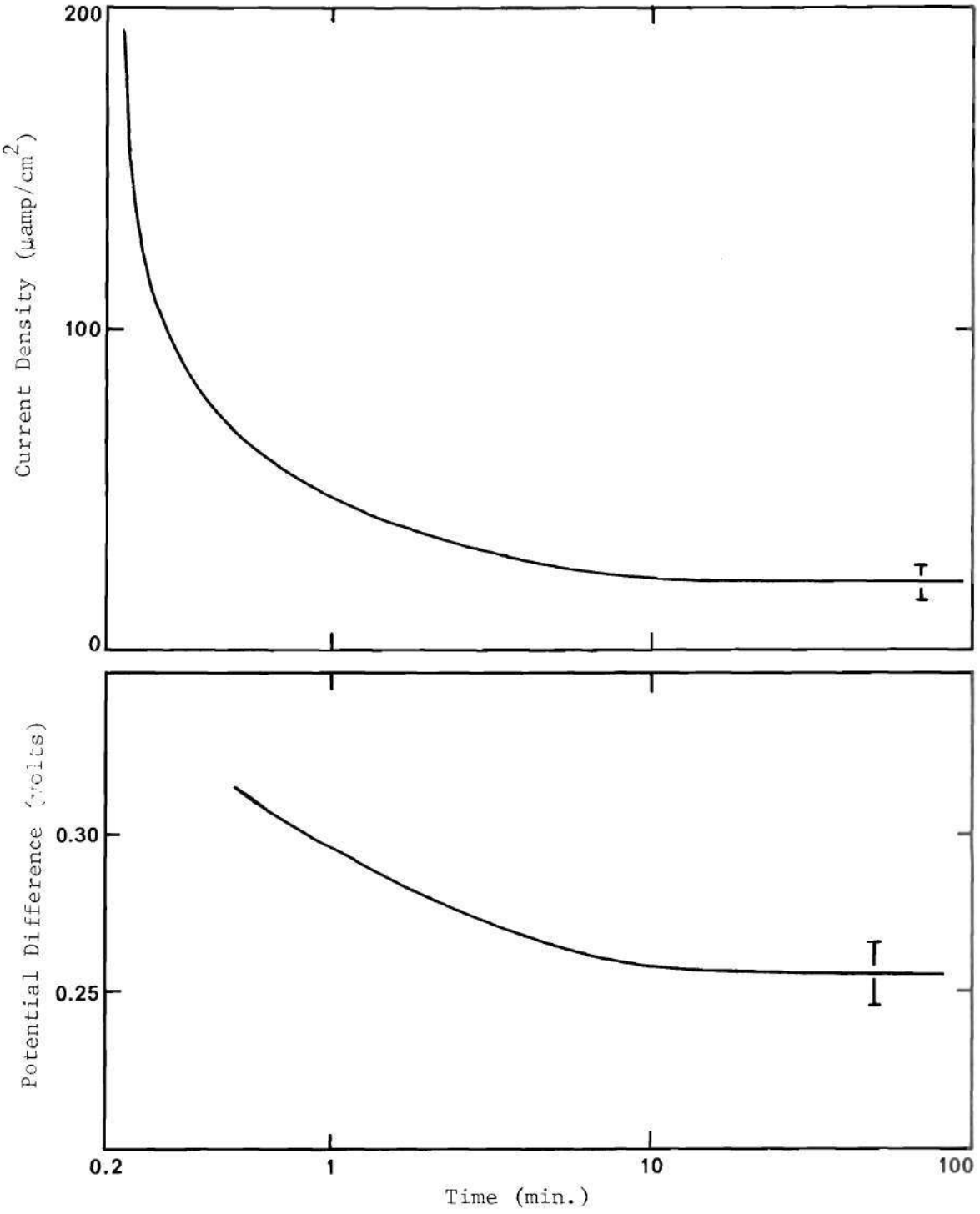

Figure 12. Equal Area Coupling Behavior in 3.5 per cent NaCl, Open to the Air: (a) Direct Coupling Current Density; (b) Open Circuit Potential Difference.

CHAPTER V

DISCUSSION OF RESULTS

Delayed failure data has been presented in terms of linear elastic fracture mechanics because this is acknowledged to be the most consistent way to quantify the mechanical conditions of cracking (39). Since the specimens had a round bottomed notch rather than a sharp crack, the static loading conditions were based on K_x rather than K_{I_c}. The round bottomed notch was chosen because its root could be adequately plated. In general, valid plane strain specimens are considered to be very desirable for stress corrosion and hydrogen embrittlement testing (39) and the specimens for this work satisfied the current dimensional requirements for plane strain except for crack length and crack sharpness. For sharply cracked samples the upper and lower critical stress intensities shown in figure 3 would be shifted to substantially lower values.

Estimates of K_{I_c} from fracture surface measurements of stress corrosion samples, designated K_{I_δ}, were made for 4340 by Peterson, et al. (32). Their calculations were based on the relative areas of slow crack growth and fast fracture. But the values obtained from such calculations will be reasonable only if the slow crack growth region is planar and crack front is straight and nearly parallel to the notch root. Since none of the specimens in this work had such attributes, the method could not be used. Another way to obtain K_{I_δ} was sought, and since the shearlip measurement and plastic zone size calculations for K_x had been found to

be in good agreement, the shearlips were examined closely for evidence of a distinction between slow crack growth and fast fracture. In several specimens with large areas of slow crack growth, the shearlip on the side of deepest hydrogen embrittlement (HE) crack penetration widened rapidly at the end of the HE region. This was assumed to be a sufficiently sharp delineation of the onset of fast fracture and sample K_{I_δ} calculations were made based on the shearlip width just before the widening (from a 20X macrograph) and the plastic zone size equation given in Chapter IV. Values of K_{I_δ} obtained in this manner ranged from 56 to 58 ksi $\sqrt{in}$, which is in good agreement with reported values for K_{I_c}.

There have been reports in the literature of complete disappearance of shearlips adjacent to hydrogen embrittlement (HE) fractures. This phenomenon is probably an indication of the stress intensity during early HE crack growth. If the shear process zone is of a subcritical size, thought to be on the order of grain size, shearlips do not form and the fracture appears to be completely plane strain. Thus, if the stress intensity is very low or the grain size is very large, shearlips will not be seen.

Fractographic studies revealed a narrow band of high plasticity adjacent to the shearlip, as shown in figure 13. The fracture surface in this region consisted mainly of elongated [shear or tear (43)] dimples, but there were also some equiaxed dimples and a few quasi-cleavage facets. The high degree of plasticity in this region was attributed to an influence of the adjacent shear process zone. The width of the band was not systematically measured, however, it should be related to the stress intensity in the same manner as the shear process zone

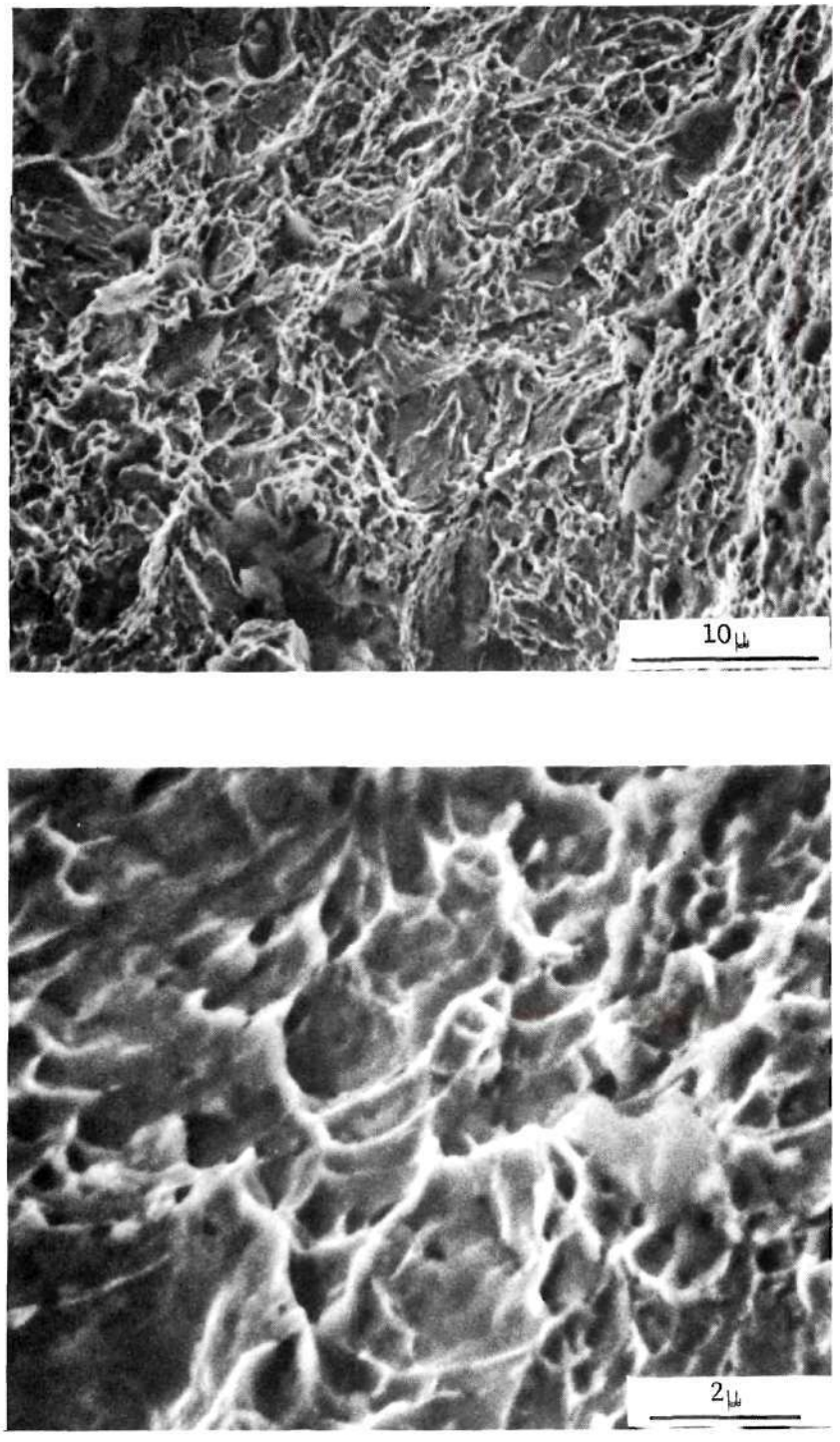

Figure 13. Scanning Electron Micrographs of the Band of Dimple Rupture Adjacent to the Shearlips: (a) High Stress Intensity Region (Part of the Shearlip Visible at the Right); (b) Elongated Dimples at Low Stress Intensity.

size (plastic zone size at a free surface, as previously calculated). Beachem (44) reported finding such a band, which he called transition to flat fracture. He found its width to be from 10 to 100 microns, but no correlation to stress intensity was made. Recently, Beachem (7) has found a region of microvoid coalescence (MVC) in hydrogen embrittlement samples at very high stress intensities. Here, he has apparently neglected his previous finding of MVC adjacent to shearlips, since for his specimens the shear process zones plus the transition region noted should be expected to occupy the entire specimen width at such high stress intensities.

Considering the intersection of the cathodic polarization curve for the steel with the anodic polarization curve for cadmium in the aerated test solution as the corrosion determining junction of an Evans diagram, the predicted corrosion current density would be about 240 $\mu a/cm^2$ (see Figure 10). The first recorded point of the direct coupling current curve (about 10 seconds after immersion) was near that value. Considering the polarization curves for the deaerated solution in like manner, the predicted corrosion current density would be about 20 $\mu a/cm^2$, which is the quasi-steady value of direct coupling current density. Since the solution was merely open to the air and neither actively aerated nor stirred during the direct coupling experiments, it is probable that the solution in the immediate vicinity of the cathode (steel) was quickly depleted of oxygen. The initial current density, then, apparently represents the sum of the cathodic processes of oxygen reduction and hydrogen evolution, while for the quasi-steady value the hydrogen reaction is controlling. The pH of the testing solution was between 6.9

and 7.0. Pourbaix diagrams (45) for iron and cadmium indicate that hydrogen evolution on the steel and corrosion of the cadmium are thermodynamically feasible for the test conditions. Although oxygen in the solution contained within the pores in the electrodeposit is probably quickly depleted, the rate of hydrogen absorption by the steel may be greatest during the time of concurrent oxygen reduction and hydrogen evolution,since oxygen at the surface is thought to facilitate entry of atomic hydrogen into steel (4).

The high ratio of cadmium surface area to exposed steel area for the plated samples would tend to indicate that the free potential of these samples would be very close to that of cadmium. The substantial difference in the initial potentials of cadmium and the plated specimens, seen in Figure 11, was attributed to the chromic acid passivation treatment performed after plating. There was a rise in the potential of cadmium after a long period of exposure to the NaCl solution. This rise was probably due to film formation and it raised the potential near that of the plated samples. The long time required for formation of a film was thought to be largely a result of the rather high hydrogen overpotential of cadmium (45,46).

The plated samples were stored in a dessicator for almost two months before testing began. Some of the hydrogen from plating probably escaped from the unbaked samples during this time (5,47). Unfortunately, there were not enough specimens to allow testing for delayed failure of as-plated samples in air; therefore, it is not known whether there was enough residual hydrogen in these specimens to cause cracking. There was little doubt, however, that the as-plated samples still contained more

residual hydrogen from plating than did the baked samples.

Examination of the electrodeposit revealed a significant increase of porosity due to baking. Some agglomeration apparently occurred in the clusters of cadmium platelets, and the baking treatment was consequently likened to a sintering of the plating. The baking temperature (475°K) was 80 percent of the melting point of cadmium, which is a fairly high relative temperature even for sintering of powder metal compacts (48); therefore, the observation of agglomeration was readily explained. The extent of exposure of the steel was not great even after baking, however, the increase in the steel to cadmium area ratio due to baking was apparently significant. The free potentials of baked and as-plated samples would not be expected to differ greatly and experiments showed that they did not. Current measurements for the freely corroding plated samples were not possible, but if cathodic current density may be assumed constant, then the total corrosion current would be substantially greater in the case of baked samples. This increase in current should result in a greater hydrogen supply per volume of underlying steel. The significantly shorter times to failure for baked specimens than for as-plated specimens in the NaCl solution (at stress intensity levels between the upper and lower critical limits) was interpreted as supporting the hypothesis that the sacrificial corrosion of the cadmium plating promotes failure by hydrogen embrittlement.

While this work was not directed toward settling the controversy over the hydrogen embrittlement mechanism, the investigation of some theoretical points was stimulated during the course of the project. One of these points was the question of whether stress assisted diffusion of

hydrogen is a factor in HE. Troiano and his co-workers (20,21) have been among the chief proponents of the theory that hydrogen diffuses rapidly along a stress gradient and ultimately concentrates in the region of highest triaxial stress. Many investigators have contested this model for hydrogen movement, but their arguments rest almost entirely on measurements of the effect of stress on hydrogen permeation of thin foils. However, such experiments do not contain the primary element of the stress assisted diffusion model, namely the stress gradient. The permeation studies can, at best, only show the effect of a gross stress and they are additionally hindered by the fact that permeation measurements include the entrance and exit rates of the hydrogen, which can be complex processes in themselves (40-42). The belief that such measurements are pertinent seems to be based on the facilitation of hydrogen movement by expansion of the lattice due to stress. The expanded lattice, however, really represents the end point of the proposed stress assisted diffusion process and not its path. Permeation measurements, then, are clearly inapplicable to an evaluation of the stress assisted diffusion model.

CHAPTER VI

CONCLUSIONS

1. Notched cantilever bending specimens of AISI 4340 steel quenched and tempered to the 260 to 280 ksi strength level and coated with a porous cadmium electroplate, were susceptible to hydrogen induced delayed failure in aqueous 3.5 per cent NaCl, whether tested as-plated or following a 23 hour baking treatment at 395°F.

2. The baked specimens, described in conclusion one, were not found susceptible to hydrogen induced delayed failure when tested in a laboratory air environment.

3. Baking at 395°F caused an increase in the porosity of the cadmium plating, which originally consisted of clusters of small platelets.

4. Electrochemical studies indicated that porous cadmium plating on tempered 4340 steel sacrifically corrodes in aqueous 3.5 per cent NaCl and that this corrosion reaction promotes hydrogen induced delayed failure of the steel.

5. Crack initiation for hydrogen induced delayed failure was found to be subsurface.

CHAPTER VII

RECOMMENDATIONS

1. Further investigation of hydrogen induced delayed failure of cadmium plated high strength steel in NaCl solutions should include testing of unplated samples coupled to cadmium anodes and unplated samples freely corroding.

2. The effect of large cadmium to steel area ratios on coupling behavior should be studied.

BIBLIOGRAPHY

1. C. A. Zapffe and C. E. Sims, Trans. AIME 145, p. 225 (1941).
2. R. W. Buzzard and H. E. Cleaves, NBS Circular 511 (1951).
3. M. L. Hill, Hydrogen Embrittlement in Metal Finishing, p. 46, Reinhold, New York (1961).
4. M. Smialowski, Hydrogen in Steel, Pergamon Press, New York (1962).
5. A. R. Elsea and E. E. Fletcher, DMIC Report 196 (1964).
6. G. T. Sink, Douglas Paper 5377 (1969).
7. C. D. Beachem, Met. Trans. 3, p. 437 (1972).
8. C. A. Zapffe and M. E. Haslem, Trans. AIME 167, p. 281 (1946).
9. P. Bastien and P. Azou, Proc. First World Metallurgical Congress, p. 535, ASM, Cleveland (1952).
10. F. deKazinczy, J. Iron and Steel Inst. 177, p. 85 (1954).
11. F. deKazinczy, Acta Met. 7, p. 525 (1959).
12. F. Garafalo, Y. T. Chou, and V. Ambegaokar, Acta Met. 8, p. 504 (1960).
13. F. deKazinczy, TVF 32, No. 3, p. 159 (1961).
14. A. S. Tetelman and W. D. Robertson, Trans. AIME 224, p. 775 (1962).
15. B. A. Bilby and J. Hewitt, Acta Met. 10, p. 587 (1962).
16. N. J. Petch and P. Stables, Nature, 169, No. 4307, p. 842 (1952).
17. N. J.Petch, Phil. Mag. Ser. 8 1, No. 4, p. 331 (1956).
18. R. P. Frohmberg, W. J. Barnett, and A. R. Troiano, Trans. ASM, 47, p. 892 (1955).
19. J. G. Morlet, H. H. Johnson, and A. R. Troiano, J. Iron and Steel Inst. 189, p. 37 (1958).
20. H. H. Johnson, J. G. Morlet, and A. R. Troiano, Trans AIME 212, p. 528 (1958).

21. E. A. Steigerwald, F. W. Schaller, and A. R. Troiano, Trans. AIME 215, p. 1048 (1959).

22. P. A. Blanchard and A. R. Troiano, WADC TR-59-444 (1959).

23. E. A. Steigerwald, F. W. Schaller, and A. R. Troiano, Trans. AIME 218, p. 932 (1960).

24. C. A. Zapffe and M. E. Haslem, Trans. ASM 39, p. 241 (1947).

25. B. F. Brown, NRL Report 4829 (1956).

26. W. L. Cotton, Plating 47, p. 169 (1960).

27. N. M. Geyer, G. W. Lawless, and B. Cohen, Hydrogen Embrittlement in Metal Finishing, p. 109, Reinhold, New York (1961).

28. D. J. Cash and W. Scheuerman, Metal Progress 75, No. 2, p. 90 (1959).

29. L. Zanker and J. Yahalom, Corrosion Sci. 9, p. 157 (1969).

30. W. F. Hamilton and M. Levine, Hydrogen Embrittlement in Metal Finishing, p. 166, Reinhold, New York (1961).

31. H. J. Read, Hydrogen Embrittlement in Metal Finishing, p. 183, Reinhold, New York (1961).

32. M. H. Peterson, B. F. Brown, R. L. Newbegin, and R. E. Groover, Corrosion 23, p. 142 (1967).

33. S. M. Toy, Corrosion 22, p. 229 (1966).

34. B. F. Brown, Mat. Res. and Stds. 6, p. 129 (1966).

35. ASTM, Mat. Res. and Stds. 1, p. 389 (1961).

36. A. S. Tetelman and A. J. McEvily, Jr., Fracture of Structural Materials, Wiley, New York (1967).

37. W. F. Brown and J. E. Strawley, Plane Strain Crack Toughness Testing of High Strength Metallic Materials, STP 410, ASTM-NASA, Baltimore (1966).

38. E. A. Steigerwald, Proc. ASTM 60, p. 750 (1960).

39. B. F. Brown, Met. Reviews, Review No. 129, p. 171 (1968).

40. R. J. Barton, Hydrogen Embrittlement in Metal Finishing, p. 20, Reinhold, New York (1961).

41. C. A. Snavely, Hydrogen Embrittlement in Metal Finishing, p. 81, Reinhold, New York (1961).

42. D. O. Hayward and B. M. W. Trapnell, Chemisorption, Butterworths, London, (1964).

43. C. D. Beachem and R. M. N. Pelloux, Fracture Toughness Testing and Its Applications, STP 381, ASTM-NASA, Baltimore (1965).

44. C. D. Beachem, Journal of Basic Engineering 87, p. 299 (1965).

45. M. Pourbaix, Atlas of Electrochemical in Aqueous Solutions, Pergamon Press, New York (1966).

46. O. Gatty and E. C. R. Spooner, The Electrode Potential Behavior of Corroding Metals in Aqueous Solutions, Oxford University Press, London (1938).

47. L. S. Darken and R. P. Smith, Corrosion 5, p. 1 (1949).

48. J. S. Hirschhorn, Introduction to Powder Metallurgy, American Powder Metallurgy Institute, New York (1969).